

FINGERPRINTS OF THE PROTOSOLAR CLOUD COLLAPSE IN THE SOLAR SYSTEM: REFRAC-TORY INCLUSIONS DISTRIBUTION AND ALUMINUM-26. F. C. Pignatale^{1,2}, M. Chaussidon², E. Jacquet¹, S. Charnoz² ¹Muséum national d'Histoire naturelle, IMPMC, UMR 7590, CP52 57 rue Cuvier, 75005, Paris, France (pignatale@ipgp.fr), ²Institut de Physique du Globe de Paris-Université Paris Diderot-UMR CNRS 71541 rue Jus-sieu, 75005, Paris, France.

Introduction: Chondrites are made of a mixture of components (Ca-Al-rich inclusions (CAIs), chondrules and matrix) that experienced different thermal histories and show diverse isotopic compositions [1]. Isotopic analyses show that the most refractory components in chondrites could have formed in a very short interval of time (within ~160 kyr) from condensate precursors formed even in a shorter time (~20 kyr) [2, 3, 4]. These timescales are comparable to the assembling time of a protoplanetary disk from its collapsing parent cloud [5]. As a consequence, the formation of precursor components of chondrites could have started during the building of the disk itself. Following the model proposed by [6, 7], we studied the distribution and thermal alteration of dust (condensates, processed and pristine) of different chemical composition during their transport from the collapsing cloud to the forming disk [8]. We found that the interplay between the collapse of the Solar System parent cloud, the dynamics of gas and dust of the forming disk, the different thermal properties of the considered dust species and the location in which the dust is injected in the disk, naturally produce aggregates of components with different thermal histories. Our calculations explain the overabundance of refractory condensed species present together with pristine dust in the colder region of the outer disk, and also the very early formation of this refractory dust in agreement with the short formation timescales proposed from isotopic data.

One precious record of the protosolar collapse phase in the refractory inclusions may be ²⁶Al, a short-lived radionuclide for which the highest initial abundances (in terms of ²⁶Al/²⁷Al) have been measured in CAIs (the so-called *canonical* value, near 5.2×10^{-5}). ²⁶Al is produced in different stellar environments [9]; to date, ²⁶Al produced by Wolf-Rayet type star is the most accepted candidate source for the Solar Nebula ²⁶Al [10].

²⁶Al decays to ²⁶Mg with a half-life of ~700 kyr [10]. The variable ²⁶Al/²⁷Al ratios observed in CAIs and chondrules have been widely used to infer time differences in the formation of these components [4, 11]. An important *caveat*, however, is whether different ²⁶Al/²⁷Al ratios actually reflect time differences between components or heterogeneities in the distribution of ²⁶Al in the solar accretion disk [4, 12, and refer-

ences therein]. Indeed, discrepancies in the absolute U-Pb ages and relative Al-Mg ages of chondrules [13], and correlations between nucleosynthetic anomalies such as ⁵⁴Cr and radiogenic excesses of ²⁶Mg [14], raise the possibility of strong ²⁶Al heterogeneities in the disk. No consensus exists on this question since other observations are in favor of a homogenous distribution of ²⁶Al [15, 16, and references therein]. Here, we use the model presented in [8] to explore how ²⁶Al heterogeneities in the parent cloud of the Solar System would result in ²⁶Al variations in different dust species in the Sun's protoplanetary disk, as a function of time and distance to the Sun. In [8], refractory Al is hosted in either high-temperature solar condensates, or pristine presolar dust, or processed dust and/or condensates.

Methods: We consider that in the cloud all ²⁶Al is in refractory species. This is consistent with the injection of all ²⁶Al from an external independent source (for example a Wolf-Rayet star), gaseous stellar ²⁶Al condensing into refractories when ejected from the star [17]. We use two arbitrary ²⁶Al distributions within the cloud shown in Fig.1.

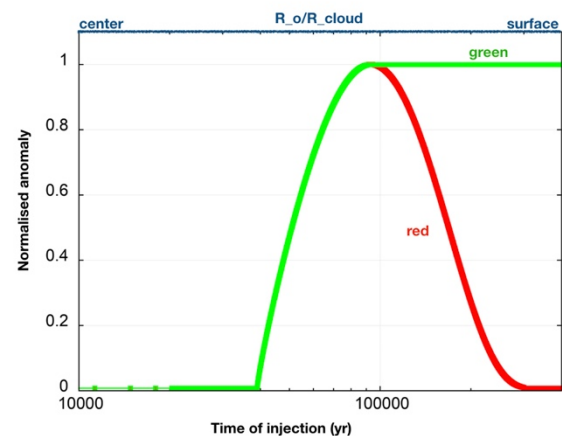


Figure 1: Chosen initial distributions of ²⁶Al in the cloud normalized to their maximum value, and time scales of injection in the forming disk.

Although arbitrary, these distributions are the two simplest possible ones imposed by the results in [8] and the fact that "normal" CAIs have canonical ²⁶Al/²⁷Al ratio. To be transported by viscous dissipation in the outer disk, where carbonaceous chondrites

likely formed, CAIs must be condensed within the first 80 kyr, from presolar material originating from the center of the presolar cloud [8]. This requires the maximum (canonical) $^{26}\text{Al}/^{27}\text{Al}$ ratio in the presolar cloud to be reached relatively close to its center (Fig. 1). The two ^{26}Al distributions considered here (Fig. 1) assume an increase from essentially zero to this value within the first 80 kyr, followed by either a decrease (red) or a plateau (green).

Results and discussion: Figure 2 shows the resulting radial distribution of $^{26}\text{Al}/^{27}\text{Al}$ in refractory condensates and in the bulk (condensates + processed dust + pristine dust) for the two chosen distributions. Both functions produce the same $^{26}\text{Al}/^{27}\text{Al}$ in refractory condensates for $R > 3$ AU, while differences are seen for $R < 3$ AU. This is due to the fact that refractory condensates also form in the inner regions at the end of the collapse inheriting the local $^{26}\text{Al}/^{27}\text{Al}$ from the gas (^{26}Al -poor for the red function, ^{27}Al -rich for the green function). A decrease in the anomaly (red function) returns high concentration of ^{26}Al for refractory condensates in the outer disk when compared with the bulk, while the constant anomaly (green function) produces bulk material with higher $^{26}\text{Al}/^{27}\text{Al}$ (this is due to the contribution of pristine material and processed pristine material to the ^{26}Al budget).

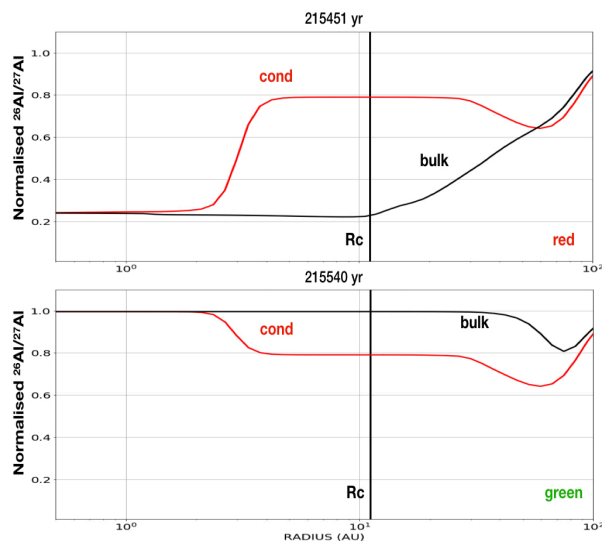


Figure 2: $^{26}\text{Al}/^{27}\text{Al}$ ratio in refractory condensates and refractory bulk (condensates + processed + pristine) at the end of the collapse ($t \sim 215$ kyr) for the red function (top) and green function (bottom).

Note that the ratios plotted in Fig. 2 are average ratios at a given heliocentric distance. In particular, the 0.8 plateau corresponds to a mix of 80 % CAIs with canonical $^{26}\text{Al}/^{27}\text{Al}$ and 20 % ^{26}Al -free CAIs having formed very early (within the first 40 kyr in Fig. 1). The proportions depend on the timing of ^{26}Al injection

(Fig. 1), that is increasing ^{26}Al earlier would increase the fraction of canonical CAIs. This scenario allows the formation of (F)UN type CAIs before the canonical CAIs, both types of CAIs being present in CV chondrites.

For the green gradient, if chondrule precursors formed in the same regions than canonical CAIs, and contemporaneously with them (see formation of silicates in [8]), chondrules will inherit a canonical $^{26}\text{Al}/^{27}\text{Al}$ ratio. Thus, the green case would predict that $^{26}\text{Al}/^{27}\text{Al}$ differences between canonical CAIs and chondrules must be ascribed to time differences in their formation. Note also that this scenario predicts that the $^{26}\text{Al}/^{27}\text{Al}$ of bulk chondrites (controlled by the mass balance between condensates, pristine and processed dusts) will be canonical, in agreement with observations [18].

In contrast, the red gradient predicts strong $^{26}\text{Al}/^{27}\text{Al}$ differences in the disk between co-located CAIs and bulk material (thus including chondrule precursors). This would rule out the use of ^{26}Al as a chronometer, but this is at variance with the observation that bulk chondrites have canonical $^{26}\text{Al}/^{27}\text{Al}$ [18].

References: [1] Scott, E.R.D., 2007, Annual Review of Earth and Planetary Sciences, 35, 577. [2] Connelly, J. N., Bizzarro, M., Krot, A. N., et al. 2012, Science, 338, 651. [3] Jacobsen, B., Yin, Q.-z., Moynier, F., et al. 2008, Earth and Planetary Science Letters, 272, 353. [4] Mishra, R. K., & Chaussidon, M. 2014, Earth and Planetary Science Letters, 390, 318. [5] Williams, J. P., & Cieza, L. A. 2011, ARA&A, 49, 67. [6] Hueso, R., & Guillot, T. 2005, A&A, 442, 703. [7] Yang, L., & Ciesla, F. J. 2012, Meteoritics and Planetary Science, 47, 99. [8] Pignatale, F.C., Charnoz, S., Chaussidon, M., Jacquet, E., 2018, ApJL, 867, L23. [9] Lugaro, M., Ott, U., Kereszturi, A., 2018, Progress in Particle and Nuclear Physics, 102, 1. [10] Dwarkadas, V.V., Dauphas, N., Meyer, B., Boyajian, P., Bojazi, M., 2017, ApJ, 851, 147. [11] Norris, T.L., Gancarz, A.J., Rokop, D.J., Thomas, K.W., 1983, Lunar and Planetary Science Conference Proceedings, 14, B331 [11] Bollard J. et al., 2017, Sci. Adv. 3, e1700407. MacPherson, G.J., Davis, A.M., Zinner, E.K., 1995, Meteoritics, 30, 365. [12] Krot, A.N., Makide, K., Nagashima, K., et al., 2012, Meteoritics and Planetary Science, 47, 1948. [14] Van Kooten E. M. M. E. et al., 2016, Proc. Natl. Acad. Sci. 113, 2011-2016. [15] Budde G. et al., 2016, Proc. Natl. Acad. Sci. 113, 2886-2891. [16] Pape J. et al., 2019, Geochim. Cosmochim. Acta 244, 416-436. [17] Pignatale, F.C., Maddison, S.T., Taquet, V., Brooks, G., Liffman, K., 2011, MNRAS, 414, 2386. [18] Schiller M., Handler M. R., Baker J. A., 2010, Earth Planet. Sci. Lett. 297, 165-173.